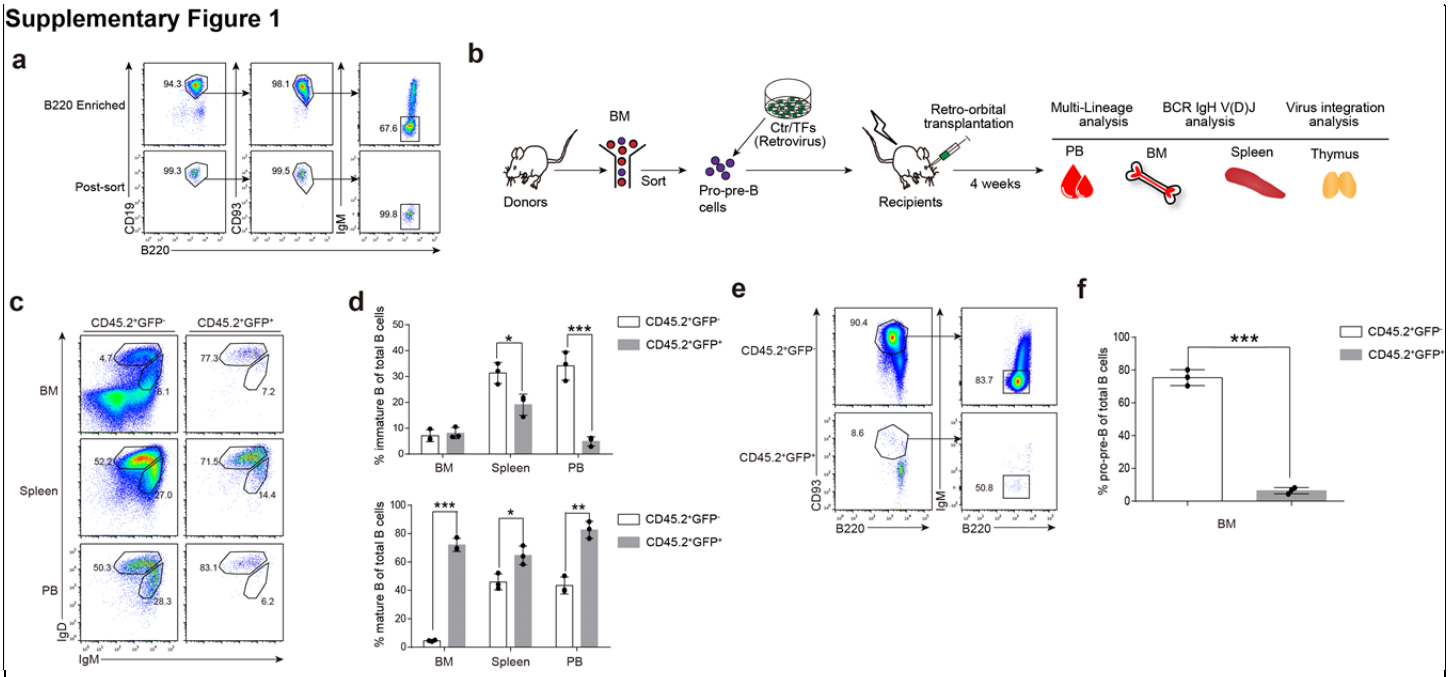

Supplementary Figure 1

Flow cytometry analysis of B cell development in recipients transplanted with 15-TF virus mixture transduced pro-pre-B cells

(a) Flow cytometry analysis of the purity of sorted Ter119$^-$Mac1$^-$CD3$^-$CD4$^-$CD8$^-$CD19$^+$B220$^+$CD93$^+$IgM$^-$ pro-pre-B cells. **(b)** Schematic diagram of 15-TF virus transduced pro-pre-B cells transplantation strategy. **(c)** Flow cytometry analysis of donor derived CD19$^+$B220$^+$IgM^{hi}IgD^{lo} immature B and CD19$^+$B220$^+$IgM^{lo}IgD^{hi} mature B cells in bone marrow (BM), spleen and peripheral blood (PB) of 15-TF pro-pre-B cell recipient mice (CD45.1$^+$ C57BL/6) four weeks post-transplantation. **(d)** Statistical analysis of immature and mature B cells in BM, Spleen, and PB. Each symbol represents an individual mouse, and small horizontal lines indicate the mean (± s.d.). *P<0.05, **P<0.01, ***P<0.001 (two-sided-independent Student's *t*-test), n = 3 biologically independent samples. **(e)** Flow cytometry analysis of donor derived CD19$^+$B220$^+$CD93$^+$IgM$^-$ pro-pre-B cells in the bone marrow of 15-TF mice. **(f)** Statistical analysis of donor derived pro-pre-B cells in BM of 15-TF pro-pre-B cell recipient mice (CD45.1$^+$ C57BL/6). Each symbol represents an individual mouse, and small horizontal lines indicate the mean (± s.d.). ***P<0.001 (two-sided-independent Student's *t*-test, n = 3 biologically independent samples). Data are representative of two independent experiments **(c, e)**.

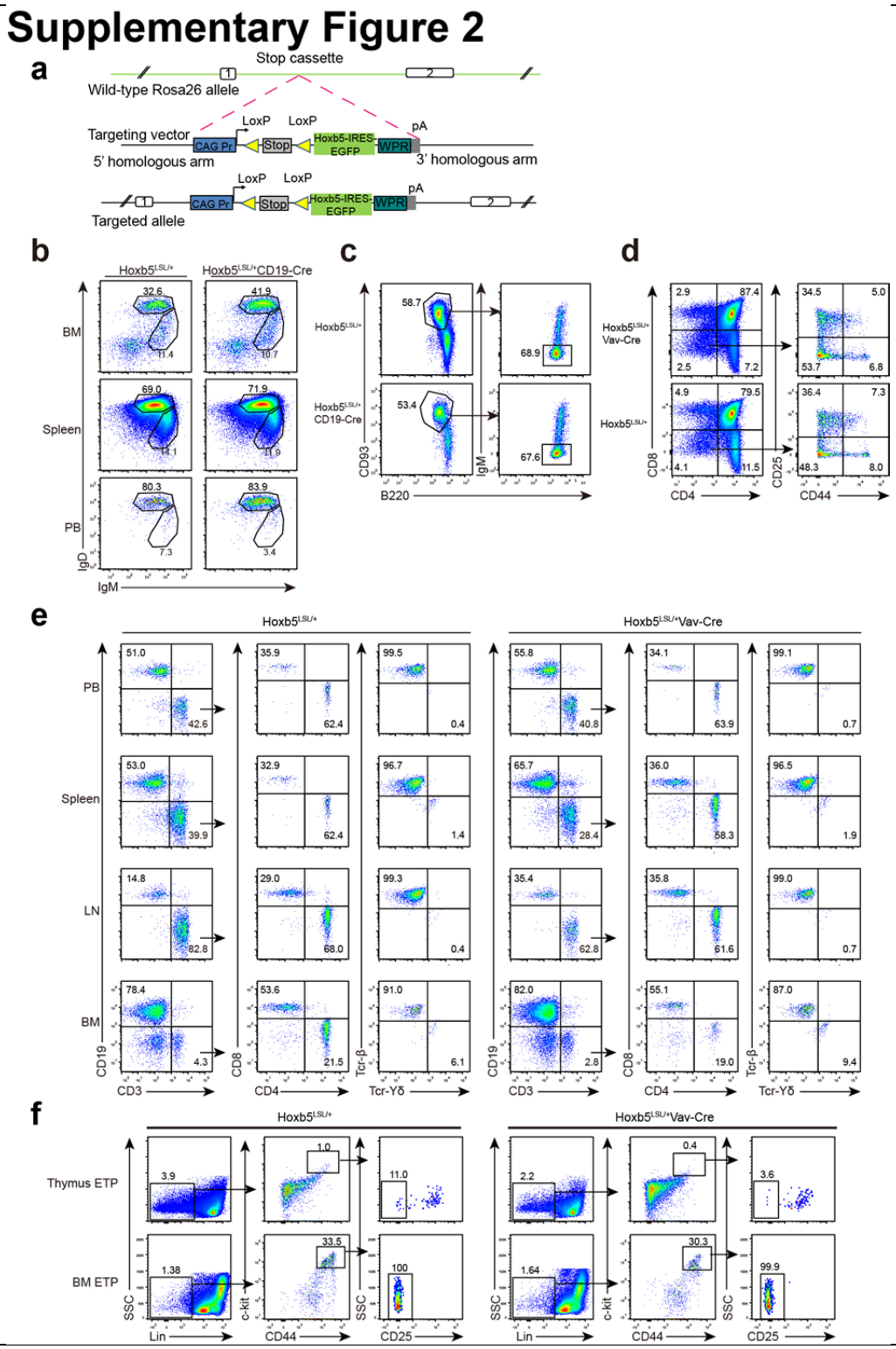

Supplementary Figure 2

Flow cytometry analysis of B and T cell development in Hoxb5-overepressing transgenic mice.

(a) Schematic diagram of Hoxb5 knock in mouse model. The Hoxb5-EGFP expression cassette was inserted into ROSA26 ($Hoxb5^{LSL/+}$ mice). **(b)** Flow cytometry analysis of $CD19^{+}B220^{+}IgM^{hi}IgD^{lo}$ immature B and $CD19^{+}B220^{+}IgM^{lo}IgD^{hi}$ mature B cells in

BM, Spleen and PB of Hoxb5$^{LSL/+}$ CD19-Cre and littermate Hoxb5$^{LSL/+}$ control mice (8-week-old). Representative plots were shown. **(c)** Flow cytometry analysis of CD19^{+}B220^{+}CD93^{+}IgM^{-} pro-pre-B cells in the bone marrow of Hoxb5$^{LSL/+}$ CD19-Cre and littermate Hoxb5$^{LSL/+}$ control mice (8-week-old). Representative plots were shown. **(d-e)** Flow cytometry analysis of DN cells in thymus **(d)** gated from Ter119^{-}Mac1^{-}CD19^{-} population, T cells in PB, Spleen, and LN **(e)** gated from Ter119^{-}Mac1^{-} population of Hoxb5$^{LSL/+}$Vav-Cre mice and littermate control (8-week-old mice). Representative plots of DN cells in thymus and T cells in PB, Spleen, LN and BM were shown. **(f)** Flow cytometry analysis of Lin^{-}CD44^{+}c-kit^{hi}CD25^{-} early T cell progenitors (ETP) in thymus and BM from the Hoxb5$^{LSL/+}$Vav-Cre mice and littermate control (8-week-old mice). Representative plots were shown. Data are representative of two independent experiments **(b-f)**.

Supplementary Figure 3

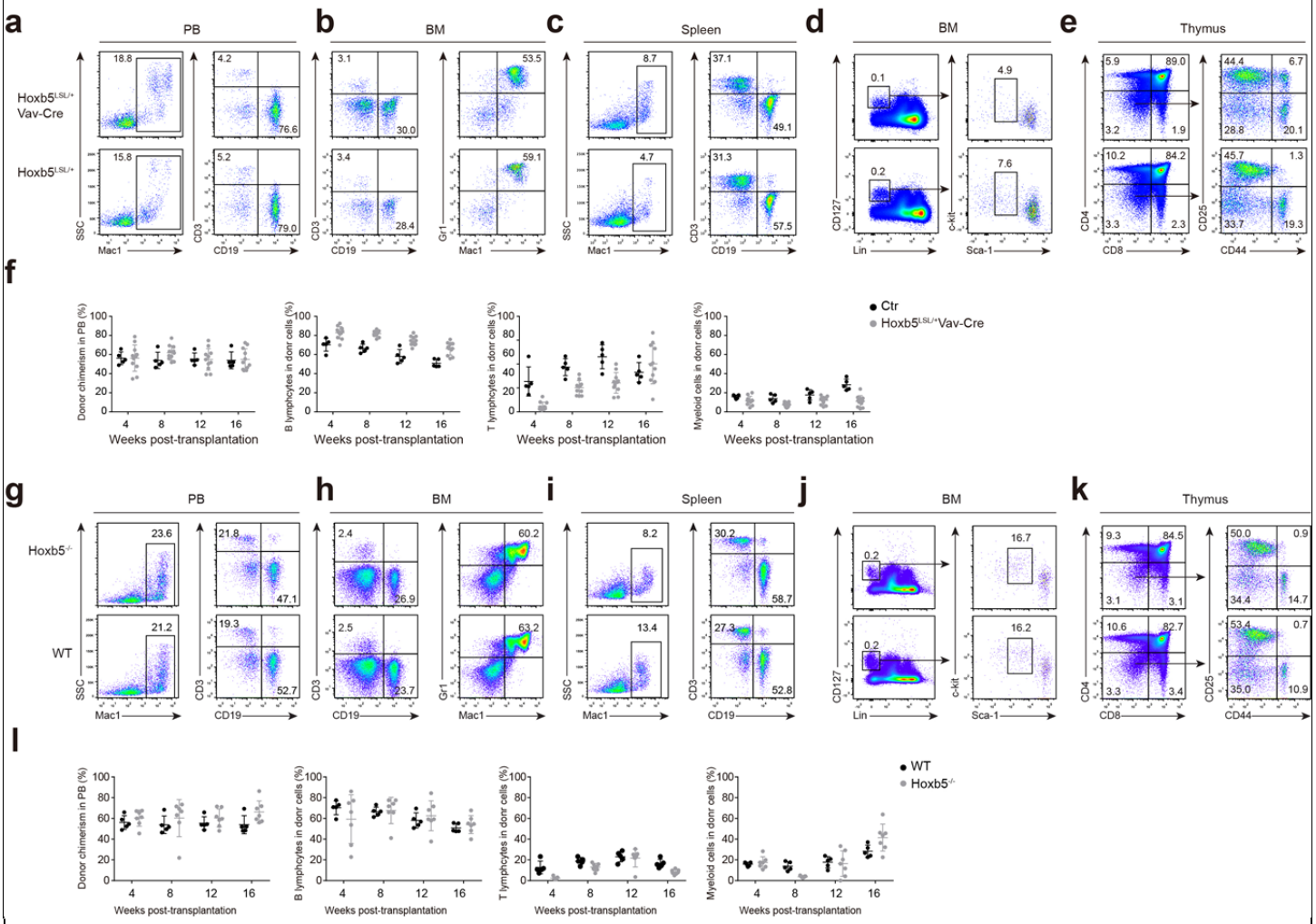

Supplementary Figure 3

Competitive bone marrow transplantation using Hoxb5-overepressing transgenic mice or Hoxb5-deficent transgenic mice as donors

(a-c) Flow cytometry analysis of hematopoietic lineages in PB **(a)**, BM **(b),** and spleen **(c)** of representative Hoxb5$^{LSL/+}$Vav-Cre and Hoxb5$^{LSL/+}$ mice (12-week-old). **(d)** Flow cytometry analysis of Lin^{-}CD127^{+}c-kit^{int}Sca-1^{int} common lymphoid progenitors (CLP) in bone marrow of representative Hoxb5$^{LSL/+}$Vav-Cre and Hoxb5$^{LSL/+}$ mice. **(e)** Flow cytometry analysis of double negative (DN) cells in thymus gated from Ter119^{-}Mac1^{-}CD19^{-}CD45.2^{+} population. Hoxb5$^{LSL/+}$Vav-Cre and Hoxb5$^{LSL/+}$ mice were analyzed. **(f)** Competitive transplantation analysis of Hoxb5$^{LSL/+}$Vav-Cre group and Hoxb5$^{LSL/+}$ (Ctr group). Half million total bone marrow cells from either Hoxb5$^{LSL/+}$Vav-Cre or Hoxb5$^{LSL/+}$ mice (CD45.2^{+}) with equivalent number of competitor cells (CD45.1^{+}) were retro-orbitally transplanted into lethally irradiated (9 Gy) individual CD45.1^{+} recipients. Donor contributions in PB of recipient mice were shown. Control group (n = 5 mice), and Hoxb5$^{LSL/+}$Vav-Cre group (n = 11 mice). Donor chimerism for total cells, Mac1^{+} myeloid cells, ,CD19^{+} B cells and CD3^{+} T cells were shown respectively. Each symbol represents an individual mouse, and small horizontal lines indicate the mean (± s.d.). **(g-i)** Flow cytometry analysis of hematopoietic lineages in PB **(g)**, BM **(h),** and spleen **(i)** of representative Hoxb5$^{-/-}$ and wild type littermate mice (12-week-old). **(j)** Flow cytometry analysis of Lin^{-}CD127^{+}c-kit^{int}Sca-1^{int} CLP in bone marrow of representative Hoxb5$^{-/-}$ and wild type littermate mice (12-week-old). **(k)** Flow cytometry analysis of DN cells in thymus gated from Ter119^{-}Mac1^{-}CD19^{-}CD45.2^{+} population of representative Hoxb5$^{-/-}$ and wild type littermate mice (12-week-old). **(l)** For competitive transplantation, half million total bone marrow cells from either Hoxb5$^{-/-}$ or WT mice (CD45.2^{+}) mice with equivalent number of competitor cells (CD45.1^{+}) were retro-orbitally transplanted into lethally irradiated (9 Gy) individual CD45.1^{+} recipients. Donor

contributions in peripheral blood of recipient mice were shown. Control group (n = 5 mice), and Hoxb5$^{-/-}$ group (n = 7 mice). Donor chimerism for total cells, Mac1^{+} myeloid cells, CD19^{+} B cells and CD3^{+} T cells were shown respectively.. Each symbol represents an individual mouse, and small horizontal lines indicate the mean (± s.d.). Data are representative of three independent experiments **(a-e, g-k)**.

Supplementary Figure 4

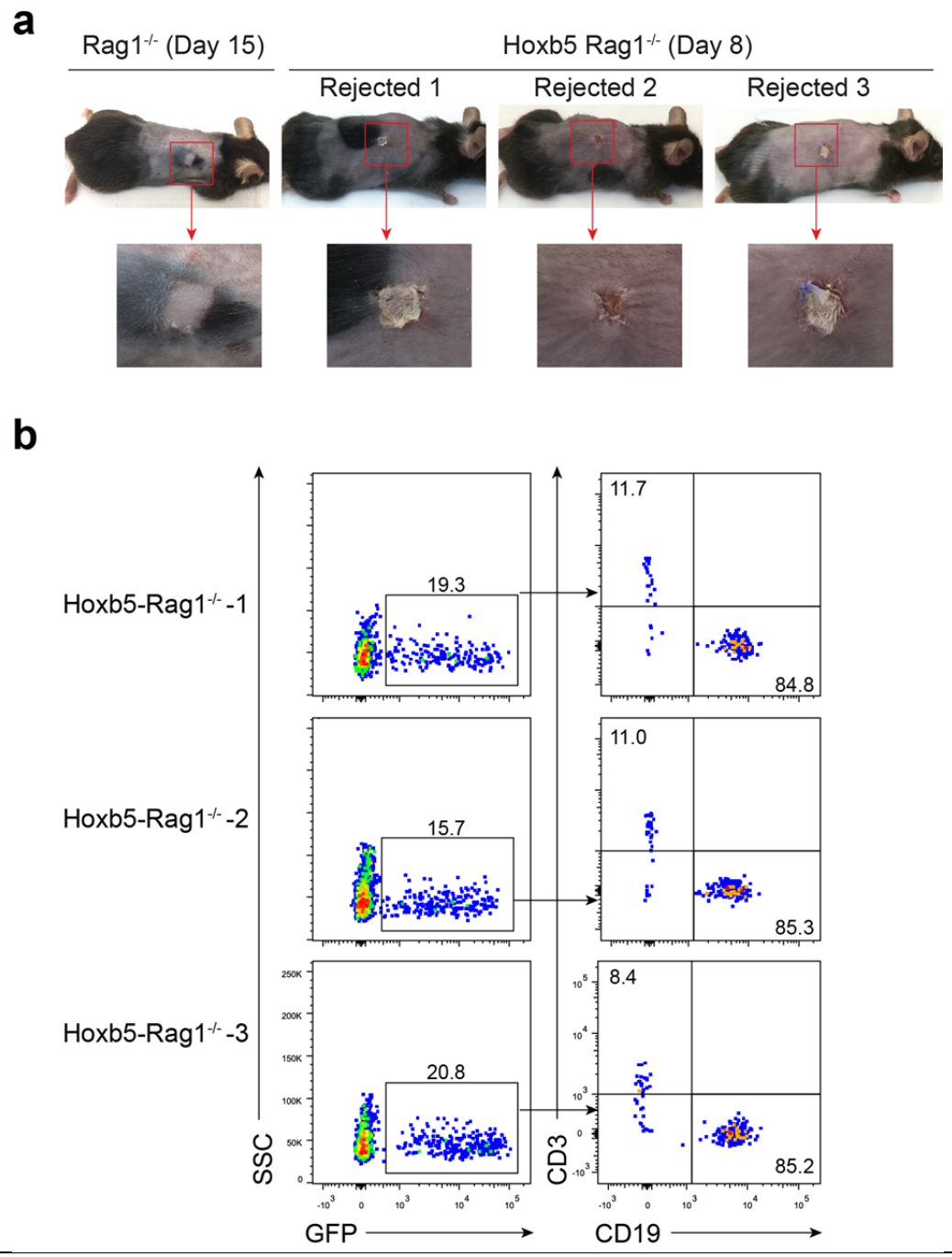

Supplementary Figure 4

iT cells generated from Rag1$^{-/-}$ mice exhibit immune functions

(a) Images of allogeneic skin-grafted Rag1$^{-/-}$ and Hoxb5-Rag1$^{-/-}$ mice. Representative images of rejected allogeneic skin tissues from three mice (day 8) and successfully grafted skin tissue control (day 15) were taken. Three weeks before the skin transplantation, three million sorted GFP^{+} pro-pre-B cells from Hoxb5$^{LSL/+}$CD19-Cre mice were transplanted into individual Rag1$^{-/-}$ mice. Donor skin

tissues were from BALB/c mice. **(b)** Three million sorted GFP^+ pro-pre-B cells from CD19-Hoxb5 transgenic mice were transplanted into individual $Rag1^{-/-}$ recipient mice lacking mature T cells. Flow cytomerty analysis of PB were performed three weeks post-transplantation. Plots of three representative recipients from ten animals of three independent experiments were shown.

Supplementary Figure 5

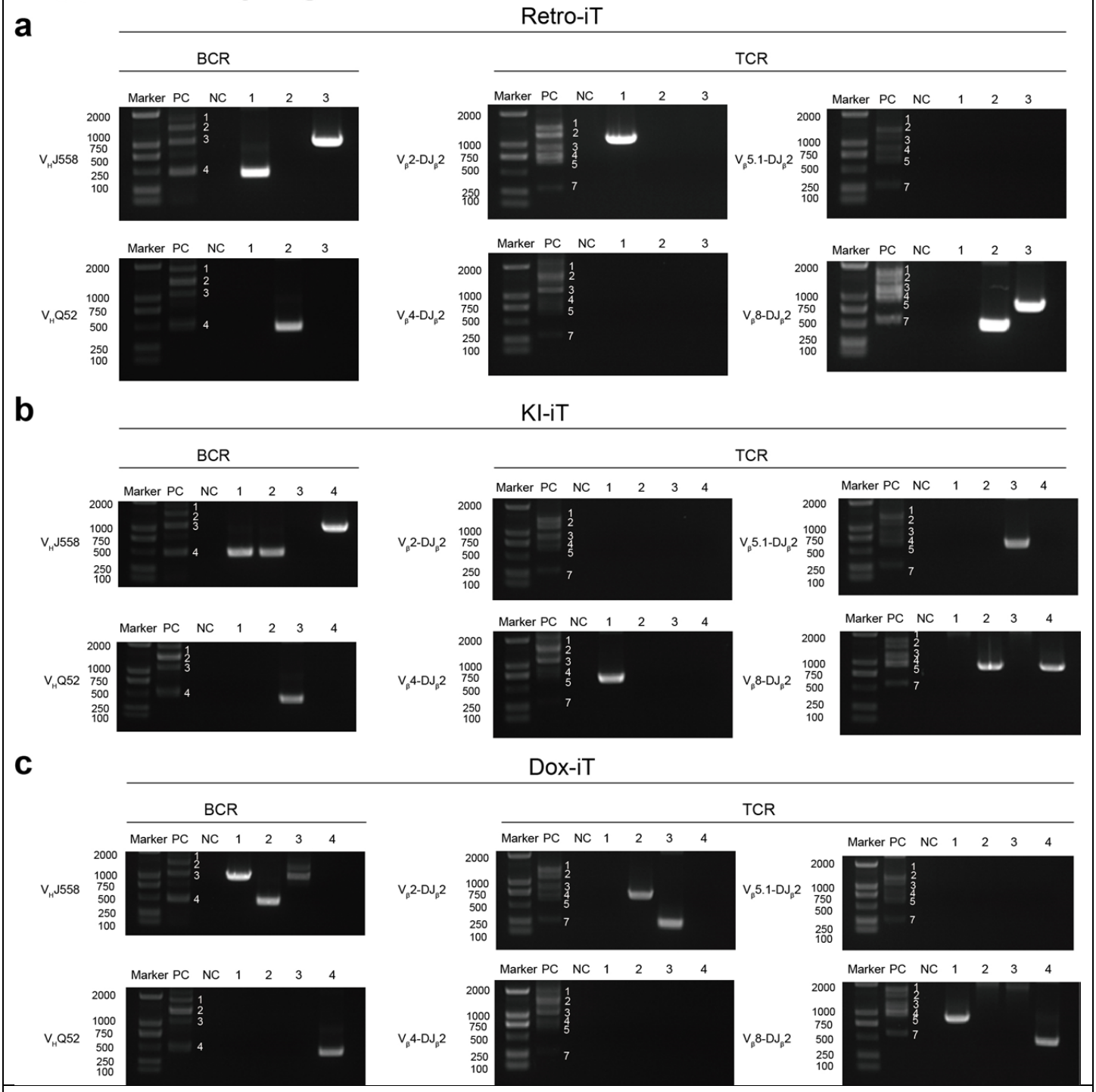

Supplementary Figure 5

PCR bands of B cell-specific BCR IgH V(D)J rearrangements and T cell-specific TCR β V(D)J rearrangements in sorted single iT cells

(a-c) PCR of B cell-specific V_HJ558 and V_HQ52 rearrangements and T cell-specific $V_\beta2$-$DJ_\beta2$, $V_\beta4$-$DJ_\beta2$, $V_\beta5.1$-$DJ_\beta2$ and $V_\beta8$-$J_\beta2$ rearrangements in sorted single iT cells of recipients transplanted with **(a)** retro-Hoxb5 pro-pre-B cells (Retro-iT), **(b)** single iT cells

of CD19-Hoxb5 pro-pre-B recipients (KI-iT) and **(c)** single iT cells of Tet-Hoxb5 pro-pre-B recipients (Dox-iT) four weeks after transplantation. Wild-type bulk pro-pre-B cells and T cells were used as positive controls (PC). Water was used as DNA template negative control to exclude DNA contaminants (NC). 200 ng DNA of each amplified single lymphocyte genome was used as template for PCR of BCR IgH V(D)J and TCRβ V(D)J rearrangements.

Supplementary Figure 6

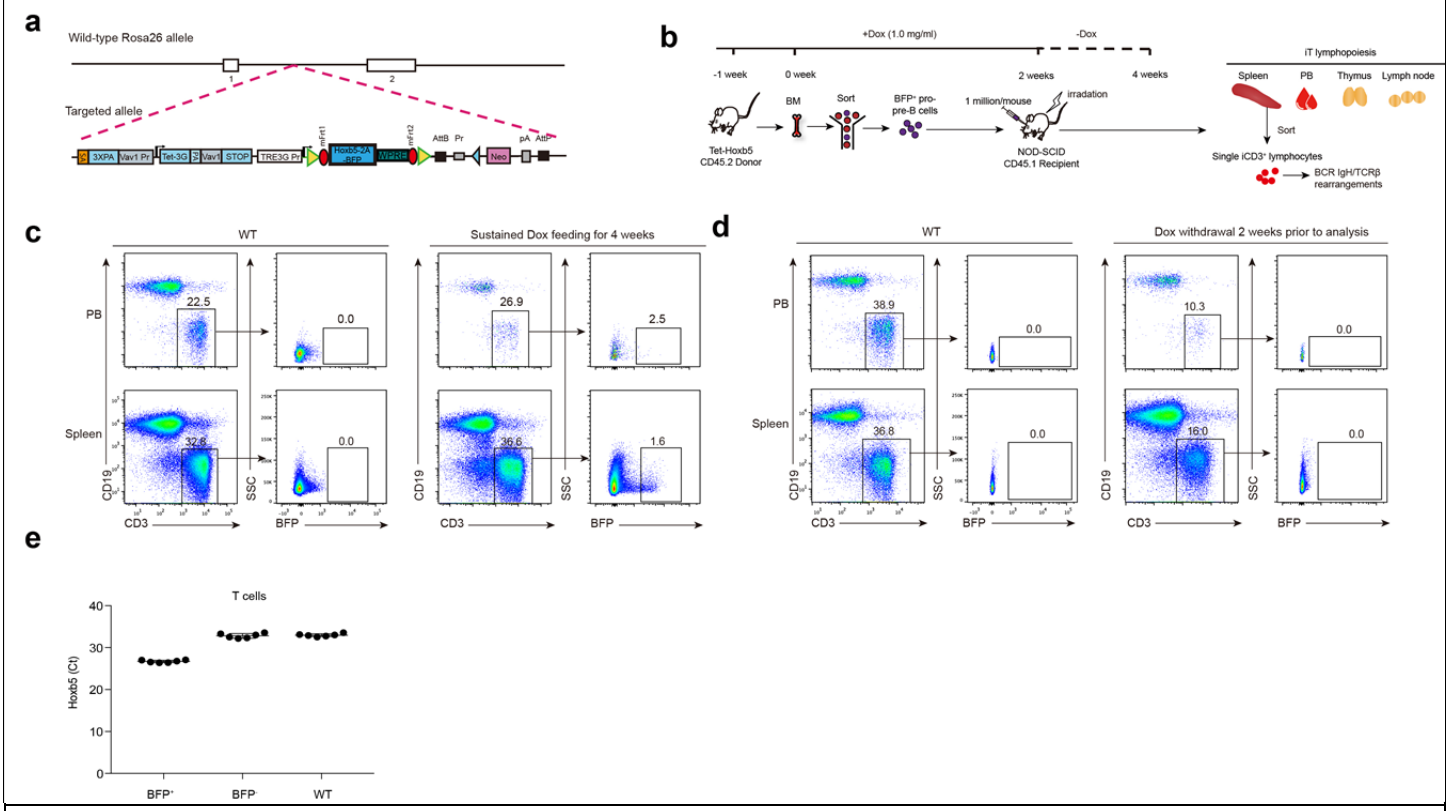

Supplementary Figure 6

Analysis of iT cells in Tet-Hoxb5 pro-pre-B recipients

(a) Schematic diagram of targeting strategy using Tet-Hoxb5 transgenic model for conditional expression of Hoxb5. The indicated expression cassette Tet-Hoxb5-BFP was inserted into ROSA26 locus. The BFP reporting Hoxb5 can be induced by Doxycycline (Dox). **(b)** Schematic strategy of B to T conversion by transient expression of Hoxb5 using Tet-Hoxb5 model. **(c-d)** Fow cytometry analysis of the iT cells gated from Ter119$^-$Mac1$^-$CD19$^-$CD45.2$^+$ in the PB and spleen of Tet-Hoxb5 pro-pre-B cell recipients maintained on Dox-water (1 mg/mL) for four weeks **(c)** and recipients maintained on conditions of Dox withdrawal 2 weeks prior to analysis **(d)**. Wild-type CD45.2 C57BL/6 mice were used as negative control. Recipient mice were analysed four weeks post-transplantation. **(e)** Q-PCR of ectopic Hoxb5 in BFP$^-$ and BFP$^+$ thymic CD3$^+$ T cells from Tet-Hoxb5-NOD-SCID mice. Wild-type CD45.2 C57BL/6 CD3$^+$ thymic T cells were used as negative control (n = 6 biologically independent samples). Data are representative of three independent experiments **(c, d)**.

Supplementary Figure 7

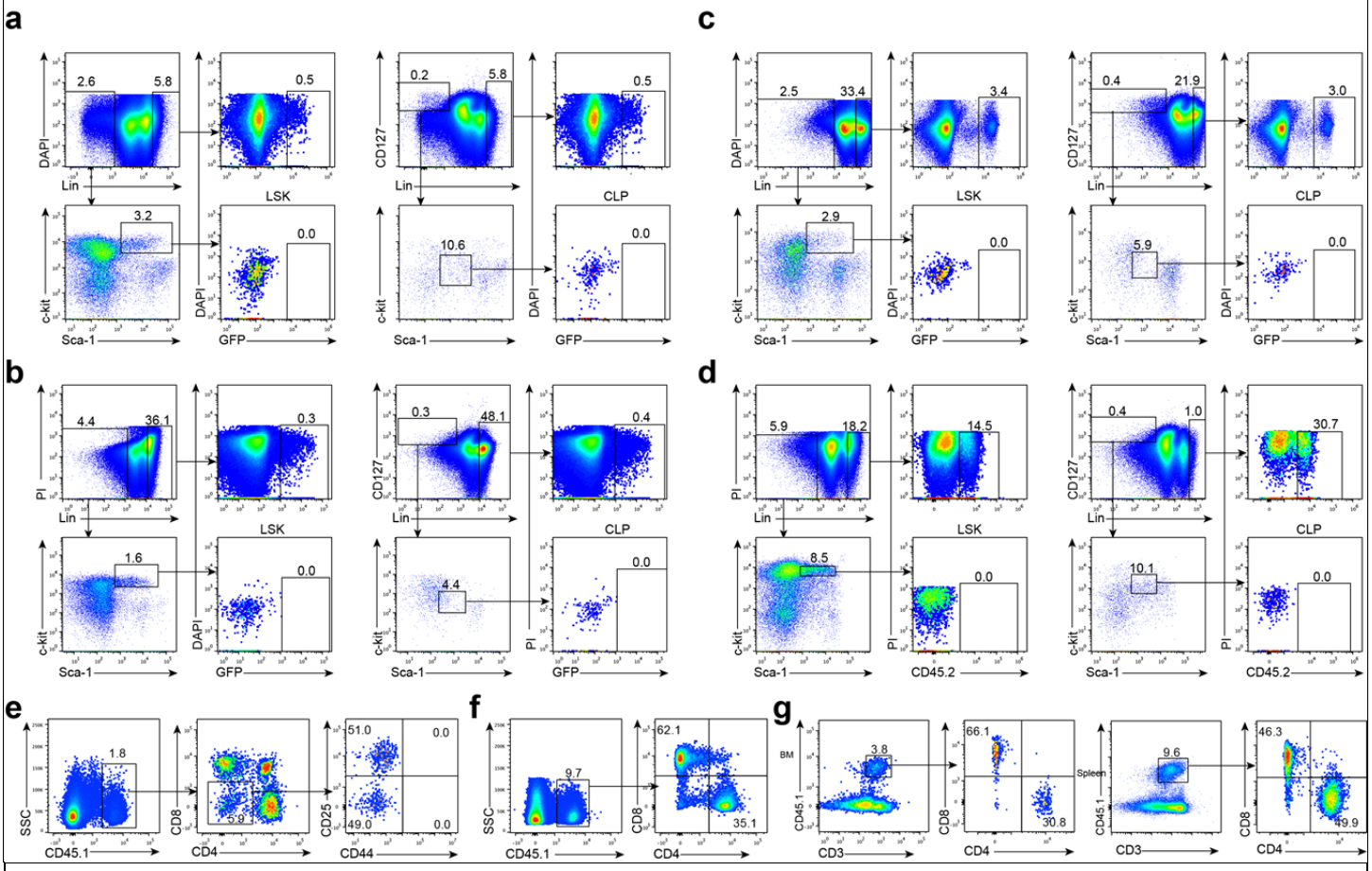

Supplementary Figure 7

Flow cytometry analysis of LSK and CLP cells in recipient mice, and T development after thymic transplantation

(a) Flow cytometry analysis of phenotypic $CD2^-CD3^-CD4^-CD8^-B220^-Mac1^-Gr1^-Ter119^-$ (Lin^-)$c\text{-}kit^+Sca\text{-}1^+$ cells (LSK) and $Lin^-CD127^+c\text{-}kit^{int}Sca\text{-}1^{int}$ (CLP) cells in the bone marrow of 15-TF pro-pre-B cell recipients. **(b)** Flow cytometry analysis were performed on phenotypic $CD2^-CD3^-CD4^-CD8^-B220^-Mac1^-Gr1^-Ter119^-$ (Lin^-)$c\text{-}kit^+Sca\text{-}1^+$ cells (LSK) and $Lin^-CD127^+c\text{-}kit^{int}Sca\text{-}1^{int}$ (CLP) cells in the bone marrow of retro-Hoxb5 mice. **(c)** Flow cytometry analysis of phenotypic $CD2^-CD3^-CD4^-CD8^-B220^-Mac1^-Gr1^-Ter119^-$ (Lin^-) $c\text{-}kit^+Sca\text{-}1^+$ cells (LSK) and $Lin^-CD127^+c\text{-}kit^{int}Sca\text{-}1^{int}$ (CLP) cells in the bone marrow of CD19-Hoxb5 pro-pre-B cell recipient mice. **(d)** Flow cytometry analysis of phenotypic $CD2^-CD3^-CD4^-CD8^-B220^-Mac1^-Gr1^-Ter119^-$ (Lin^-)$c\text{-}kit^+Sca\text{-}1^+$ cells (LSK) and $Lin^-CD127^+c\text{-}kit^{int}Sca\text{-}1^{int}$ (CLP) cells in the bone marrow of recipients 4 weeks post-transplantation with BFP^+ Tet-Hoxb5 pro-pre-B cells. The recipient mice were maintained on drinking water containing 1 mg/ml doxycycline one day prior to transplantation and for continuous two weeks. Data are representative of three independent experiments **(a-d)**. **(e-g)** Flow cytometry analysis of DN cells in thymus **(e)** gated from $Ter119^-Mac1^-CD19^-$ population, T cells in lymph node **(f)**, spleen and bone marrow **(g)** gated from $Ter119^-Mac1^-CD19^-$ population of recipients three weeks after thymic transplantation. A quarter of total wild type thymocytes ($CD45.1^+$) were transplanted into sublethally irradiated individual recipients ($CD45.2^+$) by intra-thymus injection. Data are representative of two independent experiments **(e-g)**.

Supplementary Figure 8

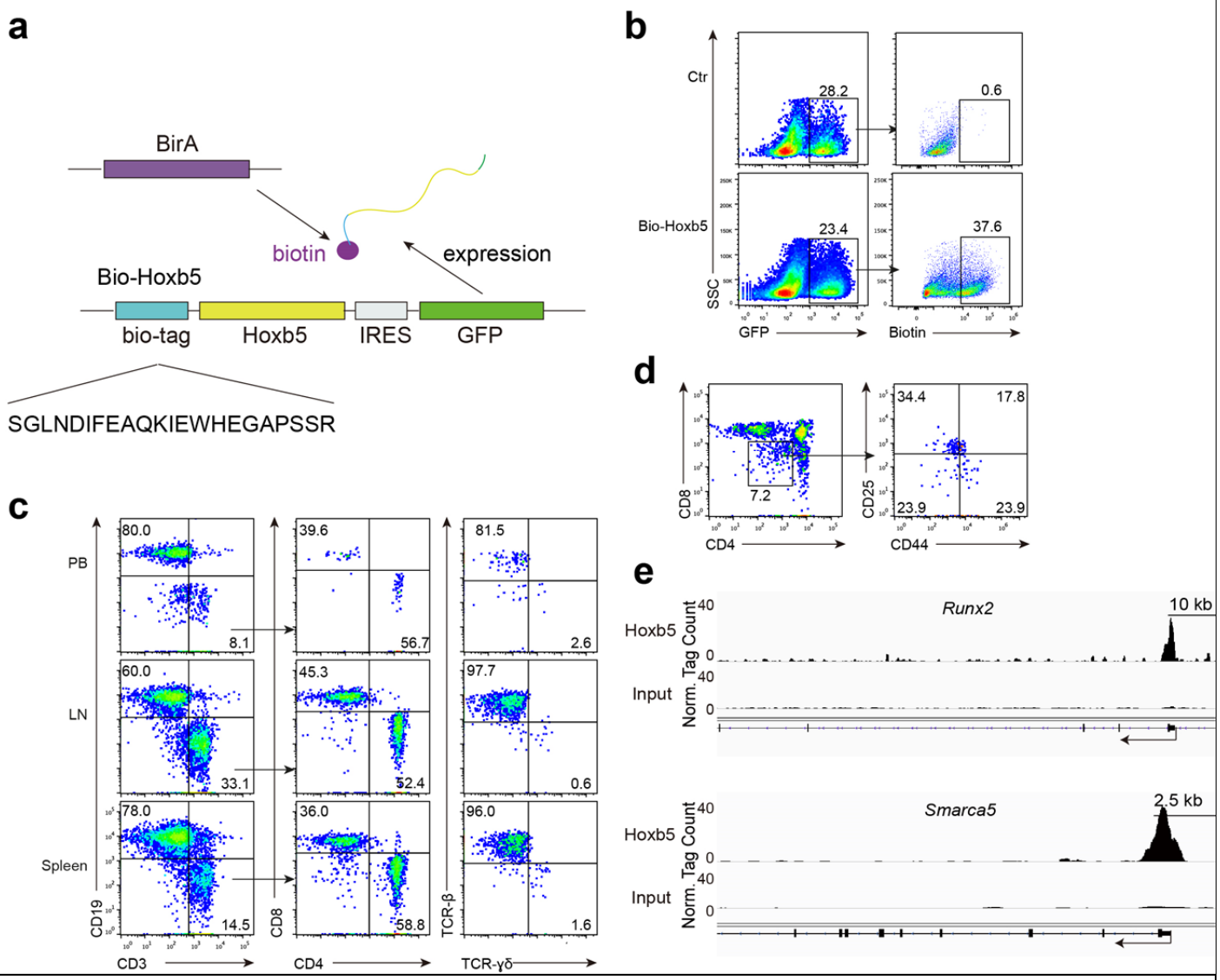

Supplementary Figure 8

Flow cytometry analysis of iT lymphocytes in Bio-Hoxb5 pro-pre-B recipient mice, and Runx2 and Smarca5 CHIP-Seq peaks

(a) Schematic diagram of Bio-tagged Hoxb5 vector cassettes. Bio-tagged Hoxb5 sequence was constructed into the pMY-IRES-GFP retro-vector. **(b)** Flow cytometry analysis of intra-cellular biotin in GFP control virus or Bio-Hoxb5 virus transduced pro-pre-B cells isolated from Rosa26$^{BirA/BirA}$ transgenic mice. Cells were analysed 72 hours post-virus transplantation. **(c-d)** Flow cytometry analysis of T cells in PB, LN and Spleen **(c)** gated from Ter119^{-}Mac1^{-}GFP^{+} population and DN cells in thymus **(d)** gated from Ter119^{-}Mac1^{-} CD19^{-} GFP^{+} population of Bio-Hoxb5 pro-pre-B recipient mice six weeks post-transplantation. **(e)** ChIP-Seq profiles Hoxb5 binding tracks in pro-pre-B on Runx2 and Smarca5 gene locus. Data are representative of two independent experiments **(b-e)**.